

Network-Centric Countermeasures Against Integrated Sensing Enabled Jamming Adversaries

Soumita Hazra and J. Harshan
Indian Institute of Technology Delhi, India

Abstract—Recent developments in Integrated Sensing and Communication have led to new adversarial models in wireless security through Integrated Sensing and Jamming (ISAJ) adversaries. ISAJ adversaries, owing to their sensing capabilities, are known to inject jamming energy over the victim’s frequency band, and also use generalized energy measurements on various network frequencies to detect the presence of countermeasures. Existing countermeasures against such ISAJ adversaries are laid under the assumption that the adversary does not have the knowledge of the countermeasure. However, according to Kerchoffs’ principle in cryptography, security of a countermeasure should only rely on the secret-keys, not on the obfuscation of the countermeasure. On testing the security of existing countermeasures, we observe that they violate Kerchoffs’ principle, thus motivating the need for new countermeasures. In this regard, we propose a novel network-centric countermeasure against ISAJ adversaries, wherein a group of users in the network assist the victim to reliably communicate her messages in a covert manner. Firstly, we analyse the error performance of the proposed countermeasure, and study its behavior on the number of assisting users in the network. Subsequently, to validate its security against Kerchoffs’ principle, we study the Shannon’s entropy associated with the presence of the victim’s messages in the network and analyse its behaviour as a function of the number of assisting users. Finally, to study the interplay between reliability and covertness, we pose interesting optimization problems and solve them to choose the underlying parameters of the countermeasure and the number of assisting users.

Index Terms—Kerchoffs’ principle, Shannon’s entropy, Jamming, ISAJ adversary, Countermeasure, Optimization.

I. INTRODUCTION

Integrated Sensing and Communication (ISAC) [1], [2] has emerged as a promising technology for 6G wireless communication networks, owing to its capability to merge sensing and communication in a single system. This integration has not only improved spectrum efficiency and reduced hardware costs, but has enabled wireless networks to act as sensors. However, in the parallel world of wireless security, recent developments in ISAC has also led to new threat models involving jamming adversaries that are enabled with integrated sensing capabilities. Such a class of adversaries, henceforth referred to as Integrated Sensing and Jamming (ISAJ) adversaries [3]–[6], intend to execute denial-of-service (DoS) [7], [8] attack on victim’s messages, by injecting jamming energy on the band, akin to traditional jammers. Furthermore, to enable the integrated sensing capabilities, ISAJ adversaries are also equipped with full-duplex radios (FDR) [9]–[11] to monitor different network frequency bands to detect the presence of potential countermeasures, while simultaneously

injecting jamming energy over the victim’s frequency band. The ISAJ adversary proposed in [4] monitors the average energy of the received symbols over the victim’s frequency band to detect the presence of countermeasures. To evade this attack, the countermeasure proposed in [4] ensures that the average energy of the received symbols over victim’s frequency band is consistent, before and after the countermeasure with a high probability. Further, [5], [6] considered a stronger ISAJ adversary, which monitors the instantaneous energy of the received symbols over all the network frequencies to detect the presence of countermeasure. Also, the ISAJ adversary compares the statistical distribution of the received symbols before and after the attack using Kullback-Leibler divergence based detector. To tackle this ISAJ adversary, the countermeasures proposed in [5], [6] ensure that the instantaneous energy of the received symbols before and after the countermeasure is consistent with a high probability, along with maintaining the statistical distribution of the received symbols over all the network frequencies.

A. Motivation

We highlight that the countermeasures proposed in [4]–[6] are laid under the assumption that the ISAJ adversary monitors the statistics of the network frequencies without the knowledge of the countermeasure. However, according to Kerchoffs’ principle in cryptography [12], for a countermeasure to be secure, details of the countermeasure should be made public, except the secret-keys. In other words, security of a countermeasure should not rely on the obfuscation of the countermeasure, rather it should rely only on the secret-keys. As a result, it is imperative to test if the countermeasures in [5], [6] remain secure when their details are made public. Towards that direction, we recall that in [5], [6], the victim is asked to move to another frequency band that is unknown to the ISAJ adversary, therein the victim and the helper, cooperatively transmit their information symbols to the destination using a new modulation technique. When the countermeasure is made public, the ISAJ adversary knows that the victim has moved to some other frequency, and is using a specific modulation technique to communicate her messages. However, the ISAJ adversary does not know the frequency band of the helper node. As a result, the uncertainty, which is quantified by Shannon’s residual entropy [13], associated with the helper’s frequency band before observing the network frequencies is $\log_2(L - 1)$ bits, where L is the total number of frequency bands. For the countermeasures in [5], [6] to be secure as per

Kerchoffs' principle, the amount of uncertainty associated with the helper's frequency band should be close to $\log_2(L-1)$ bits even after observing all the network frequencies. However, we observe that when the countermeasures in [5], [6] are implemented, the ISAJ adversary can tune into all the network frequencies to detect the specific modulation technique of the countermeasure. Owing to the fact that there is no change in the modulation techniques of the other users in the network, this further implies that the residual entropy associated with the helper's frequency band will be small. As a consequence, the countermeasures in [5], [6] are not secure against Kerchoffs' principle.

B. Contribution

For the ISAJ adversary with the capabilities mentioned in [5], [6], we introduce a new threat model abiding Kerchoffs' principle wherein all the details of the prospective countermeasure should be made public, except the secret-keys. Against this threat model, we propose a novel countermeasure referred to as the Network-Centric Mitigation Strategy (NCMS), wherein, we ask the victim to move to a helper's frequency band. Subsequently, the victim and the helper cooperatively transmit their information symbols to the destination using a portion of their energies, while they pour their remaining energies over victim's band using a shared secret-key. In addition to this, to address Kerchoffs' principle, we ask some of the network's users to work in groups, and mimic the signalling waveforms over the helper's band. In particular, the users in a group, use a part of their energies to communicate their information to the destination, and use the remaining energies to mimic the transmission over the helper's band. In NCMS since the network users deviate from their regular signalling waveforms, their error performance will be impacted. As a result, we analyse the error performance of NCMS as a function of the number of users mimicking the transmission over the helper's band and the manner in which they share their energies. Subsequently, to validate the security strength as per Kerchoffs' principle, we study the covertness of the NCMS as a function of the number of users mimicking the transmission over the helper's band. First, we show that the measured residual entropy associated with the helper's band is close to the ideal entropy values, which is governed by the number of users mimicking the helper's frequency band. Therefore, to jointly achieve reliable and covert communication under such ISAJ adversaries, we solve optimization problems to find the optimal number of users that should mimic the transmissions over the helper's band, and the optimal value of energy usage for cooperation. Extensive analysis backed by thorough simulation results reveal that reliable communication can be achieved even under the stringent Kerchoffs' principle, however with acceptable degradation in the error performance compared to the baselines that violate Kerchoffs' principle.

II. SYSTEM MODEL

We consider a heterogeneous wireless network consisting of L users, as shown in Fig. 1, which communicate with a base-

station, namely Bob, using their uplink channels on orthogonal frequencies. Also, all the uplink frequencies provided to Bob are assigned to the users of the network, and as a result, the network is crowded. Additionally, some of these L users have the requirement of high-spectral efficiency on their uplink frequencies, as a result, they are equipped with an FDR with multiple-receive antennas and single-transmit antenna. However, there is no such requirement at the other users, consequently, they are not equipped with an FDR. Of these L users, one user, namely Alice, has critical information to communicate with Bob, over the frequency band, denoted as f_{AB} . Therefore, she is a potential victim of DoS attack from an ISAJ adversary. Owing to the fact that coherent modulation schemes are susceptible to pilot contamination attack from an ISAJ adversary, Alice communicates her information modulated using non-coherent On-Off keying (OOK). The rest of the $L-1$ users are not potential victims of DoS attack from an ISAJ adversary, as a result, they use a coherent modulation scheme, to communicate their information to Bob.

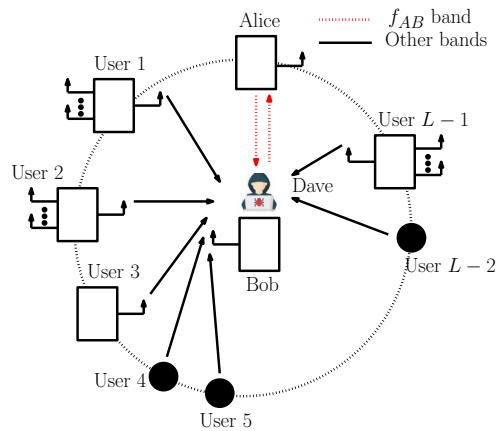


Fig. 1: Depiction of the network model, wherein Alice and the rest of the $L-1$ network users communicate with Bob, over their allocated uplink frequencies. In this network, the ISAJ adversary, namely Dave, injects jamming energy over Alice's frequency band, while monitoring different network frequencies to detect countermeasures.

Similar to [5], [6], we assume the presence of an ISAJ adversary, namely Dave, who execute DoS attack on the critical information of Alice. To achieve this, Dave injects jamming energy on the f_{AB} band, and he is also placed close to Bob so that the impact of the jamming energy is maximised. In addition to this, Dave is equipped with an FDR, as a result, he can detect the presence of potential countermeasures while injecting jamming energy on the f_{AB} band. We also assume that Dave can tune into all the network frequencies and observe the received symbols. While our threat model is similar to that in [5], [6], our main departure is the incorporation of Kerchoffs' principle, which assumes that all the details of the countermeasure is available to Dave, except the secret-keys.

A. Impact of using Kerchoffs' principle on [5], [6]

Recall that [5], [6] ask Alice to move to another frequency band, wherein Alice and the helper, cooperatively transmit

their information symbols to Bob, by using a new modulation technique. Since only one out of the $L - 1$ frequency bands undergoes changes in the modulation technique, Dave can detect this change with high probability using the knowledge of the modulation. As a consequence, he can generate a posteriori probability values on each frequency band on the likelihood of being the helper's band, and then measure the associated Shannon's residual entropy. For instance, upon implementing one such method against the countermeasure in [5], we observe that the normalised residual entropy values (measured entropy values normalized by $\log_2(L - 1)$) are upper bounded by 0.5 for $L = 42$ and SNR values of 20 dB, 25 dB, 30 dB and 35 dB. However, ideal normalised entropy is expected to be close to one, and thus we conclude that the countermeasure proposed in [5] is not secure against Kerchoffs' principle. On this note, we ask: *How to design network-centric countermeasures that are reliable and also ensure that the Shannon's residual entropy on the victim's messages in the network is within an acceptable range?*

III. NETWORK-CENTRIC MITIGATION STRATEGY

In this section, we propose a countermeasure called the Network-Centric Mitigation Strategy (NCMS), wherein we ask Alice to tune into the frequency band of a helper node in the network, referred to as Charlie, to reliably communicate her information to Bob. Further, Alice and Charlie use a part of their energies to communicate their information to Bob, and they pour their residual energies over the f_{AB} band using a shared secret-key. Assuming that Charlie, is equipped with an FDR of N_C receive-antennas and single-transmit antenna, and is communicating on the f_{CB} band, we present our strategy on the f_{CB} band and the f_{AB} band, in Section III-A and Section III-B, respectively. Now, to increase the entropy at Dave regarding the helper's frequency band, we ask L_C users of the network, for $L_C = 2c$, $c \in \mathbb{N}$, to reorganise themselves into groups of two users each, so as to mimic the signalling scheme over the f_{CB} band. These L_C users will communicate in their usual frequency band using a part of their energy, and they will pour their remaining energy into their partner's frequency band using a shared secret-key, in such a way that the signalling scheme in each of the L_C bands will mimic the signalling scheme over the f_{CB} band. For description, we assume that one such pair is formed by users namely, Tom and Henry. As the signalling scheme in their frequency bands have same structure, we will only explain the strategy over Henry's frequency band, denoted as f_{HB} band, in Section III-C.

A. Strategy over the f_{CB} band

The frame structure of information symbols over the f_{CB} band is divided across $2n$ time-slots, as shown in Fig. 2a. During the first n time slots, Alice shifts to the f_{CB} band, wherein Alice and Charlie cooperatively transmit their information symbols to Bob using a portion of their energies. In the k^{th} time-slot, where $k \in [n]$, Alice uses OOK and Charlie uses his constellation \mathcal{S} , where $\mathcal{S} \subseteq \mathbb{C}$, to transmit their information symbols to Bob. In addition to this, Alice and Charlie scale

their information symbols by $\sqrt{1 - \alpha}$ and $\sqrt{\alpha}$, respectively, where $\alpha \in (0, 1)$ represents the energy-splitting factor. The received symbol at Bob during the k^{th} time-slot, denoted using $y_{B,k}$, is given by

$$y_{B,k} = \sqrt{1 - \alpha}h_{AB,k}x_k + \sqrt{\alpha}z_k h_{CB,k} + n_{B,k}, \quad (1)$$

where $h_{AB,k} \sim \mathcal{CN}(0, 1)$ denotes the channel between Alice and Bob, $x_k \in \{0, 1\}$ denotes Alice's bits, $z_k \in \mathcal{S}$, where \mathcal{S} denotes the complex constellation used by Charlie (this could be M -PSK, M -QAM), $h_{CB,k} \sim \mathcal{CN}(0, 1)$ is the channel between Charlie and Bob, $n_{B,k} \sim \mathcal{CN}(0, N_0)$ is the additive white Gaussian noise (AWGN) at Bob, and the subscript k denotes the k^{th} time-slot. As Alice is the victim node, it is imperative to communicate her bits with utmost reliability. As a result, Charlie, who is equipped with an FDR, listens to Alice's transmitted bit while transmitting his symbol during the k^{th} time-slot, such that the received vector at Charlie, denoted using $y_{C,k}$, is given by

$$rcl y_{C,k} = \sqrt{1 - \alpha}h_{AC,k}x_k + \mathbf{h}_{CC,k} + \mathbf{n}_{C,k}, \quad (2)$$

where $\mathbf{h}_{AC,k} \sim \mathcal{CN}(\mathbf{0}_{N_C}, \sigma_{AC}^2 \mathbf{I}_{N_C})$ is the $N_C \times 1$ channel between Alice and Charlie, $\mathbf{h}_{CC,k} \sim \mathcal{CN}(\mathbf{0}_{N_C}, \alpha \rho \mathbf{I}_{N_C})$ is $N_C \times 1$ loop interference (LI) channel at Charlie, and $\mathbf{n}_{C,k} \sim \mathcal{CN}(\mathbf{0}_{N_C}, N_0 \mathbf{I}_{N_C})$ is the AWGN at Charlie, $\rho \in (0, 1)$ is the LI parameter at Charlie. Consequently, Charlie decodes Alice's bit transmitted in the k^{th} time-slot, denoted using \hat{x}_k , and incorporates this decoded bit into his transmitted information symbol in the form of energy and phase modification during the $(n + k)^{th}$ time-slot. If $\hat{x}_k = 0$, Charlie adds an additional phase shift of π/M and modifies the energy to $2 - \alpha$ of his information symbol, such that the received symbol at Bob during the $(n + k)^{th}$ time-slot is given by

$$rcl y_{B,n+k} = \sqrt{2 - \alpha}h_{CB,n+k}z_{n+k}e^{\frac{j\pi}{M}} + n_{B,n+k}, \quad (3)$$

where $h_{CB,n+k} \sim \mathcal{CN}(0, 1)$ is the channel between Charlie and Bob, $z_{n+k} \in \mathcal{S}$, $\iota = \sqrt{-1}$, $n_{B,n+k} \sim \mathcal{CN}(0, N_0)$ is the AWGN at Bob, and the subscript $(n + k)$ denotes the $(n + k)^{th}$ time-slot. Conversely, if $\hat{x}_k = 1$, Charlie transmits his symbol without any modification in the energy or phase, such that

$$rcl y_{B,n+k} = h_{CB,n+k}z_{n+k} + n_{B,n+k}. \quad (4)$$

B. Strategy over the f_{AB} band

To force Dave to believe that Alice has not vacated the f_{AB} band, it is imperative to maintain OOK over the f_{AB} band. As a result, Alice and Charlie pour their residual energies of α and $1 - \alpha$, respectively, during the k^{th} time-slot using a preshared pseudo-random bit sequence, denoted using \mathbf{a} , where $\mathbf{a} = [a_1, a_2, \dots, a_n]$ and $a_k \in \{0, 1\}$. The received symbol at Dave during the k^{th} time-slot is of the form $\sqrt{\alpha}h_{AD,k}a_k + \sqrt{1 - \alpha}a_k h_{CD,k} + n_{D,k}$, where $h_{AD,k} \sim \mathcal{CN}(0, 1)$ is the channel between Alice and Dave, $h_{CD,k} \sim \mathcal{CN}(0, 1)$ is the channel between Charlie and Dave, $n_{D,k} \sim \mathcal{CN}(0, N_0)$ is AWGN at Dave. Subsequently, during

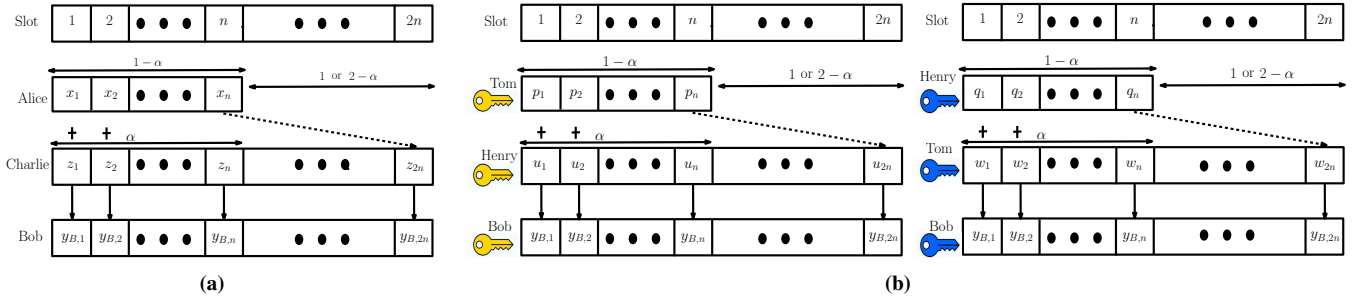


Fig. 2: The frame structure of information symbols over (a) the f_{CB} band, and (b) over the f_{HB} and the f_{TB} bands.

the $(n+k)^{th}$ time-slot, Charlie keeps silent, while Alice locally handles the formation of pseudorandom OOK sequence.

C. Strategy over the f_{HB} band

Out of the $L - 2$ users present in the network other than Alice and Charlie, we ask L_C users to form $\frac{L_C}{2}$ groups of two users each, to mimic the signalling scheme over the f_{CB} band. As shown in Fig. 2b, the users in a pair, use α energy to communicate their information to Bob, on their allocated frequency, and pour the remaining $1 - \alpha$ energy on their partner's frequency band using a secret-key. Note the secret-keys used by both the users in a pair to pour $1 - \alpha$ energy in each other's band are different, and these secret-keys are also shared with Bob. Let Tom and Henry, be one such pair who mimic the signalling scheme over the f_{CB} band. In this section, we will only explain the strategy over Henry's frequency band, i.e., the f_{HB} band, owing to the fact that signalling scheme in all the L_C frequency bands have the same structure. Tom, Henry and Bob have preshared pseudo-random bit sequence, denoted using \mathbf{p} , where $\mathbf{p} = [p_1, p_2, \dots, p_n]$ and $p_k \in \{0, 1\}$, as shown in the left figure of Fig. 2b. The contents of \mathbf{p} determine if Tom will pour energy over the f_{HB} band in the k^{th} time-slot, and also how Henry will transmit his information symbol in the $(n+k)^{th}$ time-slot. If $p_k = 1$, Tom pours $1 - \alpha$ energy over the f_{HB} band in the k^{th} time-slot, and otherwise he keeps silent, while Henry transmits his information symbol with α energy. The received symbol at Bob in k^{th} time-slot over the f_{HB} band, denoted using $y_{B,k}$, is given by

$$rcli_{y_{B,k}} = \sqrt{1 - \alpha} h_{TB,k} p_k + \sqrt{\alpha} u_k h_{HB,k} + n_{B,k}, \quad (5)$$

where $h_{TB,k} \sim \mathcal{CN}(0, 1)$ is the channel between Tom and Bob, $u_k \in \mathcal{S}$, $h_{HB,k} \sim \mathcal{CN}(0, 1)$ is the channel between Henry and Bob, $n_{B,k} \sim \mathcal{CN}(0, N_0)$ is the AWGN at Bob.¹ Furthermore, if $p_k = 1$, Henry transmits his information symbol without any modifications during the $(n+k)^{th}$ time-slot, such that the received symbol at Bob, denoted using $y_{B,n+k}$, is given by

$$rcli_{y_{B,n+k}} = h_{HB,n+k} u_{n+k} + n_{B,n+k}, \quad (6)$$

¹For the ease of notations, we use $y_{B,k}$ and $y_{B,n+k}$, to denote the received symbols at Bob, for both the f_{CB} and the f_{HB} bands.

where $h_{HB,n+k} \sim \mathcal{CN}(0, 1)$ is the channel between Henry and Bob, $u_{n+k} \in \mathcal{S}$, $n_{B,n+k} \sim \mathcal{CN}(0, N_0)$ is the AWGN at Bob. However, if $p_k = 0$, Henry adds an additional phase shift of π/M and increases the energy to $2 - \alpha$ of his information symbol, such that the received symbol at Bob during the $(n+k)^{th}$ time-slot is given by

$$rcli_{y_{B,n+k}} = \sqrt{2 - \alpha} h_{HB,n+k} u_{n+k} e^{j\frac{\pi}{M}} + n_{B,n+k}. \quad (7)$$

In the second figure of Fig. 2b, we present the frame structure of the information symbols over Tom's frequency band, denoted using f_{TB} . Here, q_k denotes preshared pseudo-random bit between Tom, Henry and Bob, and w_k denotes Tom's information symbol. From the figure, we observe that the signalling scheme of the f_{TB} band is same as that for the f_{HB} band.

IV. ERROR ANALYSIS OF NCMS

Given that the signalling method over the f_{CB} and the f_{HB} bands are different, Bob employs different decoding strategies to decode the transmitted symbols over these frequency bands. We will first discuss the decoding strategy used at Bob to retrieve the transmitted symbols over the f_{CB} band, followed by the decoding strategy at Bob to retrieve the transmitted symbols over the f_{HB} band, assuming that all the users (other than Alice), use M -ary phase-shift keying (M -PSK) to communicate with Bob.

A. Decoding strategy for symbols transmitted over f_{CB} band

Recall that, to provide reliability to Alice's information bit, we ask Charlie to embed Alice's information x_k into his transmitted symbol during the $(n+k)^{th}$ time-slot (i.e. z_{n+k}), in the form of energy and phase modifications. As a result, we conclude that the decoding strategy used at Charlie will ultimately influence the decoding strategy at Bob. First, we will discuss the decoding strategy used at Charlie to decode x_k . On the basis of the received vector $\mathbf{y}_{C,k}$, Charlie decodes Alice's information bit (\hat{x}_k) using non-coherent detection, after setting an optimal threshold τ . To achieve this, Charlie computes the energy of $\mathbf{y}_{C,k}$, denoted using $|\mathbf{y}_{C,k}|^2$, and compares it with τ . If $|\mathbf{y}_{C,k}|^2 > \tau$, then $\hat{x}_k = 1$, otherwise, $\hat{x}_k = 0$. For this decision rule, the crossover probabilities, i.e. the probabilities associated with decoding bit-0 as bit-1, and bit-1 as bit-0, are represented using P_{01} and P_{10} , respectively. As stated earlier, the decoding strategy at Bob depends on the

$$rcl\hat{r}_k, \hat{s}_k, \hat{s}_{n+k} = \arg \max_{r_k, s_k, s_{n+k}} f \left(y_{B,k}, y_{B,n+k} | x_k = r_k, z_k = e^{-\frac{i2\pi s_k}{M}}, z_{n+k} = e^{-\frac{i2\pi s_{n+k}}{M}}, h_{CB,k}, h_{CB,n+k} \right) \quad (8)$$

$$P_{e_{th1}}^{cb} = \frac{2(C_{11} + C_{13} + V_{11} + V_{13}) + C_{12} + V_{12} + C_{14} + V_{14}}{2}, \quad P_{e_{th1}}^{hb} = \frac{2(C_{11} + C_{13}) + C_{12} + C_{14}}{2} \quad (9)$$

$$rclP_{e_{th2}}^{cb} = \frac{1}{2}[2P_{11}(V_{21} + C_{21}) + 2P_{00}(V_{21} + C_{22}) + (P_{01} + P_{10})(1 - V_{21})], \quad P_{e_{th2}}^{hb} = \frac{2(C_{21} + C_{22}) + V_{22} + V_{23}}{2} \quad (10)$$

$$rclC_{11} = \sum_{i=1}^3 \frac{k_i}{\frac{t_i \alpha}{N_0} + 1}, \quad C_{12} = \sum_{i=1}^3 \frac{k_i}{\frac{2t_i \alpha}{N_0} + 1}, \quad C_{13} = \sum_{i=1}^3 \frac{k_i}{\frac{t_i \alpha}{N_{1b}} + 1}, \quad C_{14} = \sum_{i=1}^3 \frac{k_i}{\frac{2t_i \alpha}{N_{1b}} + 1}, \quad V_{13} = \left(\frac{N_{1b} \sqrt{\alpha}}{(1 - \alpha)^2} + 1 \right)^{-1} \quad (11)$$

$$rclV_{14} = \left(\frac{N_{1b} \sqrt{2\alpha}}{(1 - \alpha)^2} + 1 \right)^{-1}, \quad V_{11} = \left(\frac{N_0}{N_{1b}} \right)^{\frac{N_{1b}}{1 - \alpha}} V_{13}, \quad V_{12} = \left(\frac{N_0}{N_{1b}} \right)^{\frac{N_{1b}}{1 - \alpha}} V_{14}, \quad C_{21} = \sum_{i=1}^3 \frac{k_i}{\frac{t_i}{2N_0} + 1} \quad (12)$$

$$rclC_{22} = \sum_{i=1}^3 \frac{k_i}{\frac{t_i(2 - \alpha)}{N_0} + 1}, \quad V_{21} = \sum_{i=1}^3 \frac{k_i}{\frac{t_i}{2N_0} + 1}, \quad V_{22} = \sum_{i=1}^3 \frac{k_i}{\frac{2t_i(2 - \alpha)}{N_0} + 1}, \quad V_{23} = \sum_{i=1}^3 \frac{k_i}{\frac{2t_i}{N_0} + 1} \quad (13)$$

decoding strategy at Charlie, as a result, the values of P_{01} and P_{10} are preshared with Bob using a secret-key.

Now we will discuss the decoding strategy at Bob used to decode the transmitted symbols over the f_{CB} band. To jointly decode Alice's and Charlie's information symbols transmitted during k^{th} and $(n+k)^{th}$ time-slot, Bob uses Joint Maximum A Posteriori (JMAP) decoder, such that the decoding metric is given by (8), where $f(y_{B,k}, y_{B,n+k} | x_k, z_k, z_{n+k}, h_{CB,k}, h_{CB,n+k})$ denotes the conditional probability density function (CPDF) associated with $y_{B,k}$ and $y_{B,n+k}$, given $x_k, z_k, z_{n+k}, h_{CB,k}$ and $h_{CB,n+k}$. Here, $r_k \in \{0, 1\}$ and $s_k, s_{n+k} \in \{0, 1, \dots, M-1\}$ denote the search space of the JMAP decoder. Although the decoding metric given in (8) is optimal, it has the following shortcomings. First, the CPDF given in (8) consists of Gaussian mixtures, which are scaled by the probabilities of decoding error at Charlie, and the difficulties in using Gaussian mixtures are well known in the literature. Second, owing to the fact that the JMAP decoder given in (8) simultaneously decodes three symbols (x_k, z_k and z_{n+k}), the decoding complexity is $\mathcal{O}(2M^2)$, which is not desired. Based on the above-mentioned shortcomings, we conclude that deriving the expression of the probability of decoding error at Bob using the JMAP decoder proposed in (8) is intractable. Consequently, we propose a decoder, called Disjoint Decoder, whose decoding metric does not contain any Gaussian mixture, and the decoding complexity is $\mathcal{O}(2M)$. As the name suggests, in this decoder Bob decodes the information symbols transmitted during the k^{th} and $(n+k)^{th}$ time-slot independent of each other. Based on the received symbol $y_{B,k}$ during the k^{th} time-slot, Bob decodes Charlie's symbol z_k . Subsequently, based on $y_{B,n+k}$ during the $(n+k)^{th}$ time-slot, Bob decodes x_k and z_{n+k} . Now, we will discuss the decoding strategy at Bob to decode z_k , followed by the decoding strategy for x_k and z_{n+k} .

To decode z_k from $y_{B,k}$, the decoding metric at Bob is

$$rcl\hat{s}_k = \arg \max_{s_k} f \left(y_{B,k} | x_k, z_k = e^{-\frac{i2\pi s_k}{M}}, h_{CB,k} \right) \quad (14)$$

where $f(y_{B,k} | x_k, z_k, h_{CB,k})$ denotes the CPDF of $y_{B,k}$ given x_k, z_k and $h_{CB,k}$. Similarly, the decoding metric at Bob to decode z_{n+k} from $y_{B,n+k}$ is given by

$$rcl\hat{r}_k, \hat{s}_{n+k} = \arg \max_{r_k, s_{n+k}} f \left(y_{B,n+k} | x_k = r_k, z_{n+k} = e^{-\frac{i2\pi s_{n+k}}{M}}, h_{CB,n+k} \right), \quad (15)$$

where $f(y_{B,n+k} | x_k, z_{n+k}, h_{CB,n+k})$ denotes the CPDF of $y_{B,n+k}$ given x_k, z_{n+k} and $h_{CB,n+k}$.

B. Decoding strategy for symbols transmitted over f_{HB} band

Recall that based on p_k , Tom pours $1 - \alpha$ energy in the k^{th} time-slot, and Henry changes the phase and the energy of his symbol u_{n+k} in the $(n+k)^{th}$ time-slot. As a result, we conclude the received symbol at Bob during the k^{th} and the $(n+k)^{th}$, i.e., $y_{B,k}$ and $y_{B,n+k}$, respectively, are independent of each other, given the knowledge of p_k at Bob. Consequently, based on $y_{B,k}$, Bob decodes u_k in the k^{th} time-slot, and based on $y_{B,n+k}$, Bob decodes u_{n+k} in the $(n+k)^{th}$ time-slot. Note the decoding complexity at Bob to decode the symbols transmitted over f_{HB} is $\mathcal{O}(M)$. Now, we will explain the decoding strategy at Bob to decode u_k , followed by the decoding strategy for u_{n+k} .

To decode u_k from $y_{B,k}$, Bob uses MAP decoder, such that the decoding metric of the MAP decoder is given by

$$rcl\hat{u}_k = \arg \max_{u_k} f(y_{B,k} | p_k, u_k, h_{HB,k}), \quad (16)$$

where $f(y_{B,k} | p_k, u_k, h_{HB,k})$ denotes the CPDF of $y_{B,k}$ given p_k, u_k and $h_{HB,k}$, and u_k denote the search space of the MAP decoder. Similarly, to decode u_{n+k} from $y_{B,n+k}$, Bob uses MAP decoder, such that the decoding metric is given by

$$rcl\hat{u}_{n+k} = \arg \max_{u_{n+k}} f(y_{B,n+k} | p_k, u_{n+k}, h_{HB,n+k}) \quad (17)$$

where $f(y_{B,n+k} | p_k, u_{n+k}, h_{HB,n+k})$ denotes the CPDF of $y_{B,n+k}$ given p_k, u_{n+k} and $h_{HB,n+k}$, and u_{n+k} denote the search space of the MAP decoder.

C. Overall probability of decoding error at Bob

Let Pe_{AC} and Pe_H denote the average probability of decoding error at Bob associated with the f_{CB} band and the f_{HB} band, respectively, (averaged over all the channel realisations). The expression of Pe_{AC} can be obtained by computing the probability of various error events from (8), and similarly, the expression of Pe_H can be obtained by computing the probability of various error events from (16) and (17). Also, let Pe_{NH} denote the probability of decoding error at Bob associated with the users not mimicking the transmissions over the f_{CB} band, which are $L - L_C - 2$ in number, and it can be obtained using first principles. Therefore, the average probability of decoding error at Bob averaged over all the network users, denoted using Pe , is given by

$$rclPe = \frac{Pe_{AC} + L_C Pe_H + (L - L_C - 2) Pe_{NH}}{L}. \quad (18)$$

Theorem 1. An upper bound on Pe , denoted by Pe_{th} , is

$$rclPe_{th} = \frac{Pe_{th1}^{cb} + Pe_{th2}^{cb} + L_C (Pe_{th1}^{hb} + Pe_{th2}^{hb}) + 2(L - L_C - 2) Pe_{th}^{nh}}{L}.$$

Here, Pe_{th1}^{cb} , Pe_{th2}^{cb} , Pe_{th1}^{hb} and Pe_{th2}^{hb} denote the probability of decoding error using the decoding metric given in (14), (15), (16) and (17), respectively, and $P_{00} = 1 - P_{01}$ and $P_{11} = 1 - P_{10}$. Also, Pe_{th}^{nh} denotes the upper bound on probability of decoding error at Bob associated with those users who are not mimicking the transmissions over the f_{CB} band, which are $L - L_C - 2$ in number. The expression of Pe_{th1}^{cb} and Pe_{th1}^{hb} are given in (9), and Pe_{th2}^{cb} and Pe_{th2}^{hb} are given in (10), and the expression of Pe_{th}^{nh} can be derived using first principles. Also, the expressions of the variables in Pe_{th1}^{cb} , Pe_{th1}^{hb} , Pe_{th2}^{cb} and Pe_{th2}^{hb} are given in (11), (12) and (13), where $k_1 = 0.168$, $k_2 = 0.144$, $k_3 = 0.002$, $t_1 = 0.876$, $t_2 = 0.525$, $t_3 = 0.603$, $N_{1b} = N_0 + 1 - \alpha$ and $e = \sqrt{3 - \alpha - 2\sqrt{2 - \alpha}\cos(\pi/M)}$.

D. Simulation Results

To prove the correctness of the derived upper bound Pe_{th} , we fix L_C and L , and then study the behaviour of Pe_{th} and Pe , as a function of α . Owing to the fact that average probability of decoding error at Bob associated with the users not mimicking the signalling scheme over the f_{CB} band does not depend on α , for this analysis, we will only consider the average probability of decoding error associated with the f_{CB} and the f_{HB} bands, which are L_C in number. In Fig. 3, we plot Pe_{th} as a function of α , marked using magenta, for $L_C = 10$, $N_C = 4$, and at an SNR of 35 dB. In the same figure, for the same set of parameters, we use monte-carlo simulations to plot Pe as a function of α , marked using blue. From these plots, we have the following observations. First, the curve of Pe_{th} sits slightly above the curve of Pe , which validates the fact that Pe_{th} is an upper bound on Pe . Second, we observe that the curve of Pe_{th} and Pe follow a similar trend, and their minima are around the same value of α .

Next, we fix L and vary L_C , and study the behaviour of Pe as a function of SNR. In this regard, in Fig. 4, we use

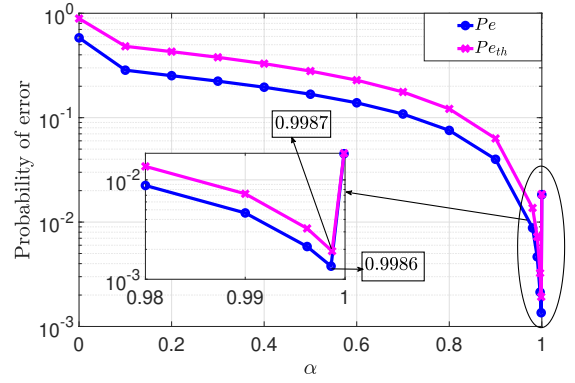


Fig. 3: Plots depicting Pe and Pe_{th} , as a function of α , for $L_C = 10$, $N_C = 4$, and at an SNR of 35 dB. We observe that the minima of Pe and Pe_{th} , are around the same value of α .

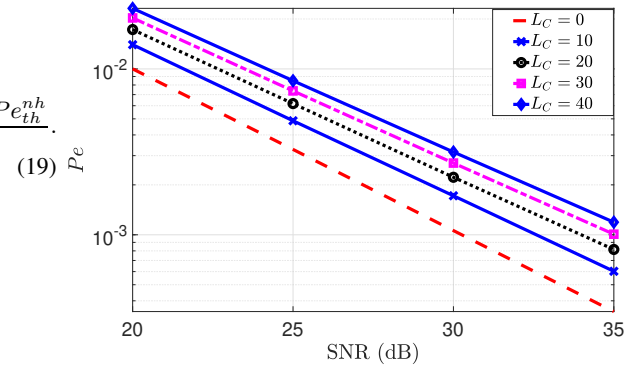


Fig. 4: Plot depicting Pe as a function of SNR, for different values of L_C and $L = 42$. From these plots, we observe that as L_C increases, Pe increases.

monte-carlo simulations to plot Pe as a function of SNR, for $L = 42$, and different values of L_C . To generate these plots, for a given L_C and SNR, we compute the operating value of α such that Pe_{th} is minimised, and substituted these values in (18), to get Pe . From these plots, we have the following observations. First, for a given L_C , Pe decreases with SNR, which is required from any reliable communication system. Second, we observe that for a given SNR, Pe increases with L_C . This is because $Pe_H > Pe_{NH}$, this is a penalty for mimicking the signalling scheme over f_{CB} band, and as L_C increases, $(L - L_C - 2)$ decreases. Stitching these two events, we conclude that as L_C increases, $L_C Pe_H$ increases, while $(L - L_C - 2) Pe_{NH}$ decreases, consequently, Pe increases.

V. COVERTNESS ANALYSIS OF NCMS

Recall that Kerchoffs' principle states that all the details about the signalling scheme should be made public, except the secret-keys. In this regard, Dave has the following knowledge about the scheme discussed in Section III. First, Dave knows that Alice has moved to an another band, to communicate her information reliably to Bob. Alice and the incumbent user of that band, pour $1 - \alpha$ and α energies, respectively, to communicate their information symbols to Bob in the k^{th} time-slot. Also, that user is equipped with an FDR, as a result,

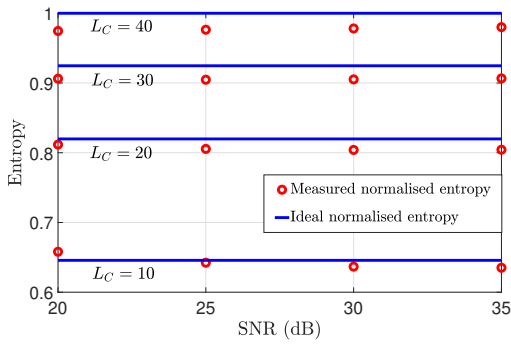


Fig. 5: Figure shows the plot of normalised entropy as a function of SNR, for different values of L_C and $L = 42$. From these plots, we observe that as L_C increases, the normalised entropy increases.

to provide an added layer of reliability to Alice's information bits, that user incorporates Alice's bits into its symbols in the form of phase and energy modifications in the $(n+k)^{th}$ time-slot.² Second, Dave knows that Alice and the incumbent user of that band, pour α and $1-\alpha$ energies, respectively, over f_{AB} band to form pseudo-random bit sequences, using a shared secret-key. Third, Dave knows the operating value of energy-splitting factor α . We highlight that although Dave knows all the details of NCMS, he does not know the band to which Alice has moved to communicate her information to Bob. As a result, his objective is to find out the helper's frequency band using the knowledge of the countermeasure.

To find out the helper's frequency band, Dave tunes into all network frequencies (except Alice's band), collects the received symbols for a frame-length of f symbols. The received symbol at Dave for a frequency band l in a given slot of frame, in the k^{th} and the $(n+k)^{th}$ time-slot, are denoted using $d_{k,l}$ and $d_{n+k,l}$, respectively, where $l \in \{1, \dots, L-1\}$. Next, Dave uses two sets of CPDF, one containing the CPDFs on countermeasure setup, and the other containing the CPDF for no countermeasure setup. The CPDF of the countermeasure setup for $x_k = 0$ and $x_k = 1$, are denoted using D_1 and D_2 , respectively, and the CPDF for no countermeasure setup is denoted using D_3 . Next, using $d_{k,l}$, $d_{n+k,l}$ and α , Dave counts the number of times D_1 or D_2 gets maximised averaged over f for a frequency l , which is denoted using m_l . Dave repeats this operation for all the $L-1$ network frequencies. Note that the higher the value of m_l , the higher the probability that the band l is the helper's frequency band. As a result, based on m_l , Dave assigns scores to all the network frequencies, denoted using P_l , by using the softmax function $P_l = \exp(dm_l)$, where d is the scaling factor. Using P_l , the entropy associated with the helper's frequency band, denoted using H , is given by

$$rclH = - \sum_{l=1}^{L-1} P_{n,l} \log_2(P_{n,l}), \quad (20)$$

where $P_{n,l}$ denotes the probability, which is given by $P_{n,l} =$

²Note that the probability of decoding error at that incumbent user associated with Alice's bits are shared with Bob using a secret-key, as a result, Dave does not know the values of P_{00} , P_{11} , P_{01} and P_{10} .

$\frac{P_l}{\sum_{l=1}^{L-1} P_l}$. The measured normalised entropy, denoted using H_{norm} , is given by $H_{norm} = \frac{H}{\log_2(L-1)}$, where $H_{norm} \in (0, 1)$, such that $H_{norm} = 0$ and $H_{norm} = 1$, correspond to no uncertainty and maximum uncertainty, respectively, regarding the helper's frequency band at Dave.

A. Simulation results

To show the security strength of NCMS in maintaining uncertainty at Dave regarding the helper's frequency band, in Fig. 5, we use monte-carlo simulations to plot the measured normalised entropy H_{norm} , for various combinations of L_C and SNR, $d = 10$, $f = 200$ and $L = 42$, along with the ideal normalised entropy, which is given by $\frac{\log_2(L_C+1)}{\log_2(L-1)}$, marked using horizontal line. Note that for a given L_C , the operating value of α is chosen in such a way that P_{eth} is minimum. From these plots, we observe that H_{norm} is close to the ideal normalised entropy, which shows the security strength of NCMS against Kerchoffs' principle. Also, we observe that as L_C increases, H_{norm} increases. This is due to the fact that as more users mimic the transmissions over the f_{CB} band, the difference in the value of normalised assigned probability $P_{n,l}$ minimises, consequently, H_{norm} increases.

Based on the discussion in this section and the preceding section, we conclude that as L_C increases, the reliability at Bob averaged over all users degrades, while the entropy at Dave regarding the helper's band improves. This suggests that there is a tradeoff between reliability and entropy, and L_C should be chosen such that the reliability is maximum, subject to the measured entropy is within an acceptable range.

VI. PARAMETER OPTIMIZATION OF NCMS

To communicate both reliably and covertly, we present an optimization problem in Problem 1, which provides the optimal value of α and L_C , denoted using α^* and L_C^* , respectively. This problem is posed such that the average probability of decoding error at Bob Pe is minimised, with the measured normalised entropy H_{norm} lower bounded by δ , for some $0 \leq \delta \leq 1$.

Problem 1. For a given L , N_C and SNR, we solve:

$$rclL_C^*, \alpha^* = \arg \min_{\alpha \in (0,1), L_C \in \{1, \dots, L-1\}} Pe, \quad (21)$$

subject to: $H_{norm} \geq \delta$.

However, given that we have an upper bound on Pe (i.e., P_{eth} , given in Theorem 1), instead of the true expression, and there is no expression of measured normalised entropy H_{norm} , we propose to solve Problem 2, which provides L_C^\dagger and α^\dagger , such that $\frac{\log_2(L_C^\dagger+1)}{\log_2(L-1)} \geq \delta$, and compare it with the solution provided by Problem 1. In Table I, we tabulate the solutions to Problem 1 and Problem 2, for different values of SNR and δ . From the table, we observe that the solutions to Problem 1 and Problem 2 are close to each other, which suggests the accuracy of modified optimization problem. From the table, we observe that for a fix L and SNR, as δ increases, L_C^* (or L_C^\dagger) increases,

TABLE I: Solutions to Problem 1 and Problem 2 for $L = 42$.

	$\delta = 0.658$		$\delta = 0.8117$		$\delta = 0.9062$		$\delta = 0.9746$	
SNR	(α^*, L_C^*)	$(\alpha^\dagger, L_C^\dagger)$						
30	(0.9970, 10)	(0.9973, 10)	(0.9978, 20)	(0.9978, 20)	(0.9978, 30)	(0.9980, 28)	(0.9981, 40)	(0.9982, 38)
	$\delta = 0.6351$		$\delta = 0.8043$		$\delta = 0.9066$		$\delta = 0.9801$	
35	(0.9986, 10)	(0.9987, 10)	(0.9988, 20)	(0.9990, 20)	(0.9990, 30)	(0.9990, 28)	(0.9991, 40)	(0.9991, 38)

consequently Pe increases. This observation is in agreement with the plots shown in Fig. 4. In Table II, we present the solutions to Problem 2, for $\delta = 0.7$, and different values of L . From the table, we observe that for a fix δ , as L increases, L_C^\dagger increases. Now, as the difference between L and L_C^\dagger increases, we observe that the contribution of $(L - L_C^\dagger - 2)Pe_{NH}$ to Pe becomes dominant (see (18)), as a result, Pe decreases with L , which is shown in Fig. 6. Thus, as L increases, the overall error performance of the network improves for a given δ .

Problem 2. For a given L , N_C and SNR, we solve:

$$rclL_C^\dagger, \alpha^\dagger = \arg \min_{\alpha \in (0,1), L_C \in \{1, \dots, L-1\}} Pe_{th}, \quad (22)$$

$$\text{subject to: } \frac{\log_2(L_C + 1)}{\log_2(L - 1)} \geq \delta.$$

TABLE II: Solutions to Problem 2 for different values of L

SNR	$L = 50$	$L = 100$	$L = 150$	$L = 200$
	$L_C^\dagger = 14$	$L_C^\dagger = 24$	$L_C^\dagger = 32$	$L_C^\dagger = 40$
20	0.9907	0.9928	0.9938	0.9946
25	0.9950	0.9959	0.9963	0.9967
30	0.9975	0.9979	0.9981	0.9983
35	0.9988	0.9990	0.9991	0.9991

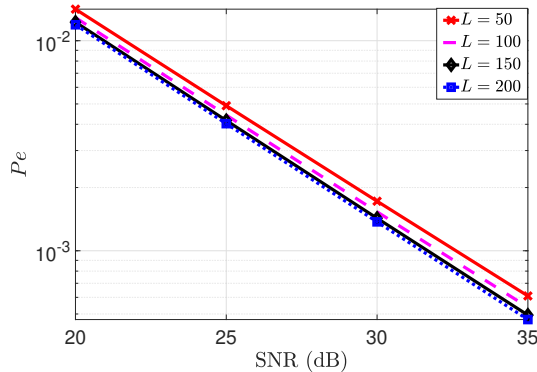


Fig. 6: Plots depicting Pe , as a function of SNR, for $\delta = 0.7$ and different values of L . To generate these plots we use Table II.

VII. COMMUNICATION OVERHEADS AND FUTURE WORK

In this section we highlight various overheads associated with NCMS from implementation aspects. Firstly, NCMS is applicable when there is no strict latency constraints on the messages of the victim node. This is because the base station takes some time-slots to make transition from the normal setup to the countermeasure setup, after realising that the

victim's band is jammed. For instance, to implement NCMS, the base-station (i) has to identify the list of users willing to participate in NCMS, (ii) form groups of two users based on their geographical locations and synchronization capabilities, and finally (iii) distribute the necessary power allocation parameters to all the participating users. Besides these overheads associated with migrating to NCMS mode, the participating users must be provided secret-keys to synchronously pour energies into their partner's frequency band. In particular, to implement NCMS, users in each pair need a key-rate of 0.5 bits per channel use of common randomness, which accounts to an overall key-rate of $\frac{L_c}{2}$ bits per channel use in the network. Given that this is the first work of its kind to propose a countermeasure against an ISAJ adversary abiding Kerchoffs' principle, we believe there are interesting research directions for future work especially addressing the problems of communication and secret-key overheads.

REFERENCES

- [1] Liu, An, et al. "A Survey on Fundamental Limits of Integrated Sensing and Communication," *IEEE Communications Surveys and Tutorials* 24.2, pp. 994-1034, 2022.
- [2] S. Lu et al., "Integrated Sensing and Communications: Recent Advances and Ten Open Challenges," in *IEEE Internet of Things Journal*, vol. 11, no. 11, pp. 19094-19120, June, 2024.
- [3] M. K. Hanawal, D. N. Nguyen and M. Krunz, "Cognitive Networks With In-Band Full-Duplex Radios: Jamming Attacks and Countermeasures," in *IEEE Trans. on Cognitive Commun. and Netw.*, vol. 6, no. 1, pp. 296-309, March 2020.
- [4] V. Chaudhary and J. Harshan, "Fast-Forward Mitigation Schemes for Cognitive Adversary," in *IEEE Trans. on Cognitive Commun. and Networking*, Vol. 07, No. 04, pp. 1304-1319, Dec. 2021.
- [5] S. Hazra and J. Harshan, "On High-Rate, Low-Overhead Mitigation Strategies Against Cognitive Adversaries," *National Conference on Communications*, Feb. 2024.
- [6] S. Hazra and J. Harshan, "On Reliable Communication under Reactive Adversaries with Generalized Energy Detectors," in *IEEE Transactions on Vehicular Technology*, Dec. 2024.
- [7] M. Chen, J. Ben-Othman and L. Mokdad, "Novel Denial-of-Service Attacks Against LoRaWAN on MAC Layer," in *IEEE Commun. Letters*, vol. 27, no. 11, pp. 3123-3126, Nov. 2023.
- [8] H. Pirayesh and H. Zeng, "Jamming Attacks and Anti-Jamming Strategies in Wireless Networks: A Comprehensive Survey," in *IEEE Commun. Surveys and Tutorials*, vol. 24, no. 2, pp. 767-809, 2022.
- [9] S.-M. Kim, Y.-G. Lim, L. Dai and C.-B. Chae, "Performance Analysis of Self-Interference Cancellation in Full-Duplex Massive MIMO Systems: Subtraction Versus Spatial Suppression," *IEEE Trans. Wireless Commun.*, vol. 22, no. 1, pp. 642-657, Jan. 2023.
- [10] Mohammadi et al., "A Comprehensive Survey on Full-Duplex Communication: Current Solutions, Future Trends, and Open Issues," *IEEE Commun. Surveys and Tutorials*, vol. 25, no. 4, pp. 2190-2244, 2023.
- [11] Z. H. Hong et al., "Frequency-Domain RF Self-Interference Cancellation for In-Band Full-Duplex Communications," in *IEEE Trans. on Wireless Commun.*, vol. 22, no. 4, pp. 2352-2363, April 2023.
- [12] A. Kerckhoffs, "La cryptographie militaire," *Journal des sciences militaires*, vol. IX, pp. 5-83, Jan. 1883, pp. 161-191, Feb. 1883.
- [13] C. E. Shannon, "A mathematical theory of communication," *Bell Syst. Tech. J.*, vol. 27, pp. 379-423, July, 1948.